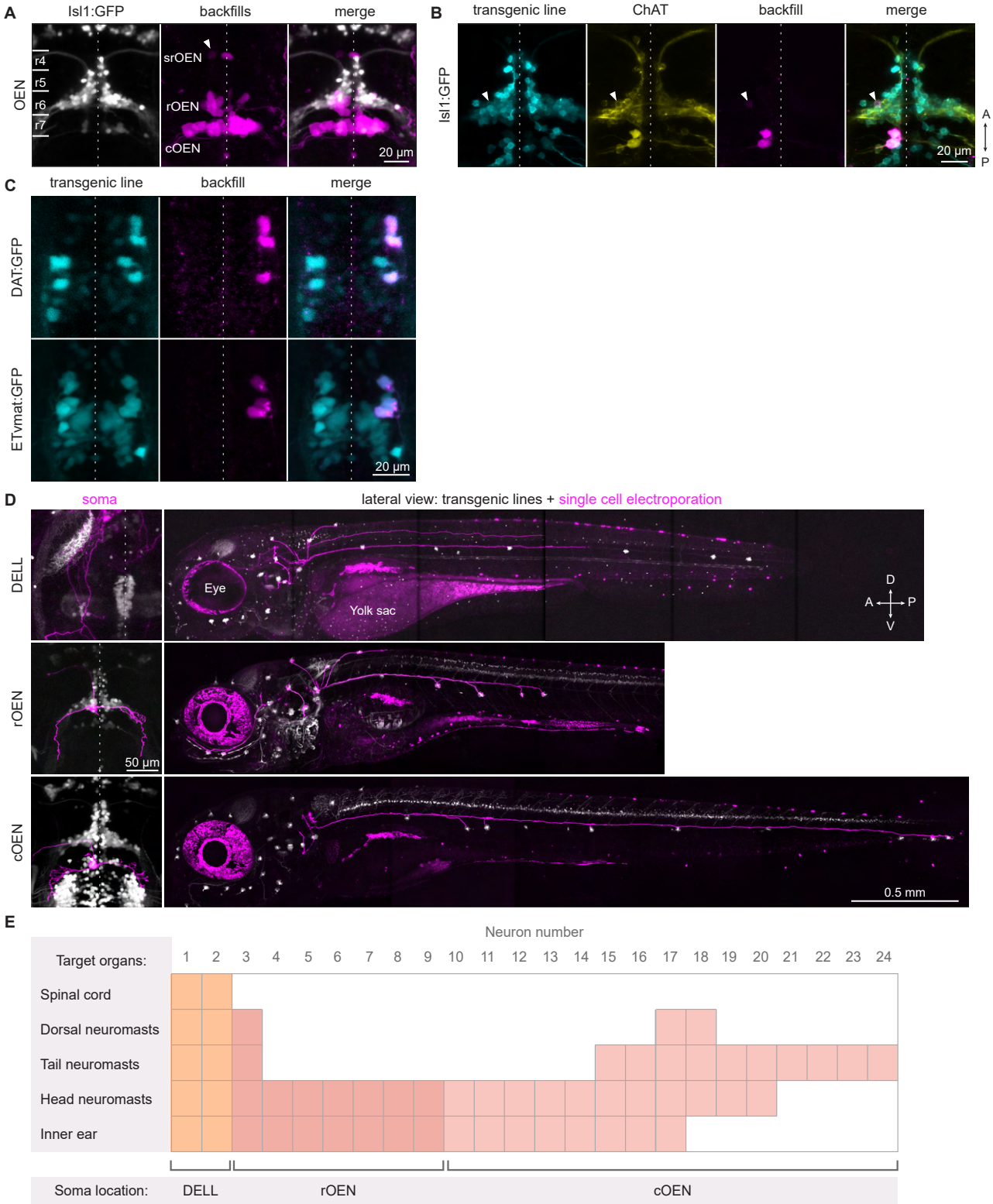
A
Isl1:GFP
backfills
merge
OEN
r4
r5
r6
r7
srOEN
rOEN
cOEN
20 µm
B
transgenic line
ChAT
backfill
merge
Isl1:GFP
A
P
20 µm
C
transgenic line
backfill
merge
DAT:GFP
ETvmat:GFP
20 µm
D
soma
lateral view: transgenic lines + single cell electroporation
DELL
Eye
Yolk sac
D
A
P
V
rOEN
50 µm
cOEN
0.5 mm
E
Neuron number
Target organs:
1 2 3 4 5 6 7 8 9 10 11 12 13 14 15 16 17 18 19 20 21 22 23 24
Spinal cord
Dorsal neuromasts
Tail neuromasts
Head neuromasts
Inner ear
Soma location:
DELL
rOEN
cOEN

Figure S1. Characterization of neurotransmitter identity and target of efferent nuclei. Related to Figure 1.
(A) Composite image showing all hindbrain neurons labeled after dye injections of the lateral line nerve in Isl1:GFP larvae. Images were registered using anatomical landmarks made visible by GFP expression. The labeled neurons occupy three distinct positions along the antero-posterior axis spanning rhombomeres r4 to r7, and are named accordingly: caudal, rostral, and supra-rostral OEN (n=17 fish, 6 bilateral). Dotted line: midline. Arrowhead: srOEN neuron. **(B)** Maximum intensity projections of confocal images of an Isl1:GFP larval hindbrain after a unilateral lateral line nerve dye injection and subsequent antibody stain against choline acetyltransferase (ChAT). Arrowhead: labeled neuron in the rOEN. **(C)** Maximum intensity projections of confocal images of the hypothalamus of transgenic larvae following unilateral lateral line nerve dye injections. Neurons labeled by the injections also express GFP under the Dopamine Active Transporter (DAT, top), and the Vesicular Monoamine Transporter (VMAT, bottom) promoters. **(D)** Focal electroporations of membrane-tagged fluorescent proteins reveal efferent neuron morphologies. Maximum intensity projections of confocal images showing the morphology of single lateral line efferent neurons. Dorsal and lateral views of single cells (magenta) electroporated in double transgenic larvae expressing GFP in all hair cells, Tg(Brn3c:GFP), and in additional lines that label the efferent nuclei (gray). Top: DELL neurons in the ETvmat2:GFP background (5 dpf). Middle/bottom: rostral and caudal OEN neurons in Isl1:GFP fish (10 and 8 dpf, respectively). We were unable to successfully label a single srOEN neuron using this technique. Note: both the eyes and the yolk sac are auto-fluorescent and therefore also appear magenta. This signal is unrelated to the electroporations. **(E)** Matrix summarizing the observed target organs of individual efferent neurons, which were made visible using single cell electroporations (n= 24 fish, one neuron per fish).

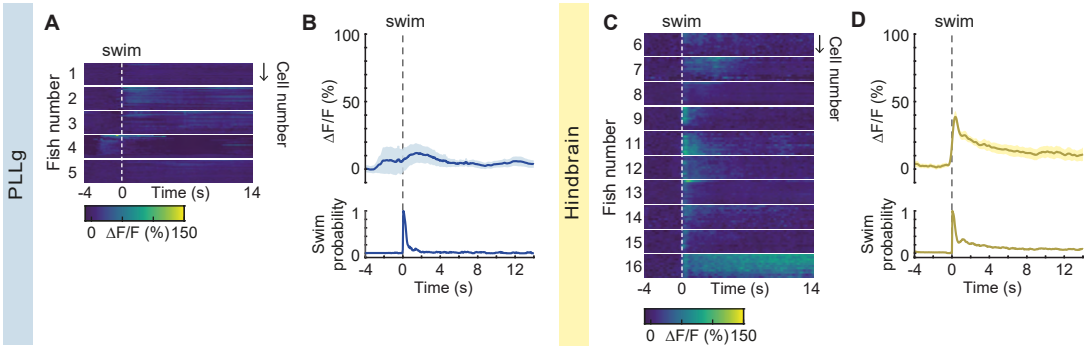

Figure S2. Activity of PLLg primary sensory neurons and hindbrain neurons during head-restrained swimming. Related to Figure 2.

(A) Average single-cell responses (ΔF/F) during spontaneous swim bouts of neurons belonging to the corresponding 5 flow-sensitive fish in Figure 2C (n= 20, 26, 16, 24, 30 cells). **(B)** Population swim-triggered averages of neuronal activity in the PLLg (mean ΔF/F ± s.e.m.). Bottom: swim probability during the same period. Averages arise from the single-cell measurements shown in Figure S2A. **(C)** Average single-cell responses (ΔF/F) of hindbrain neurons in the vicinity of the PLLg belonging to the corresponding fish in Figure 2F (n= 11 cells per fish). Note that fish 10 is missing since no hindbrain neurons were imaged in this fish. Fish 16 showed strong and prolonged hindbrain activity reflecting sustained OMR-induced swim activity. **(D)** Population swim-triggered averages of neuronal activity in hindbrain neurons (mean Δ F/F ± s.e.m.). Bottom: swim probability during the same period. Averages arise from the single-cell measurements shown in Figure S2C.

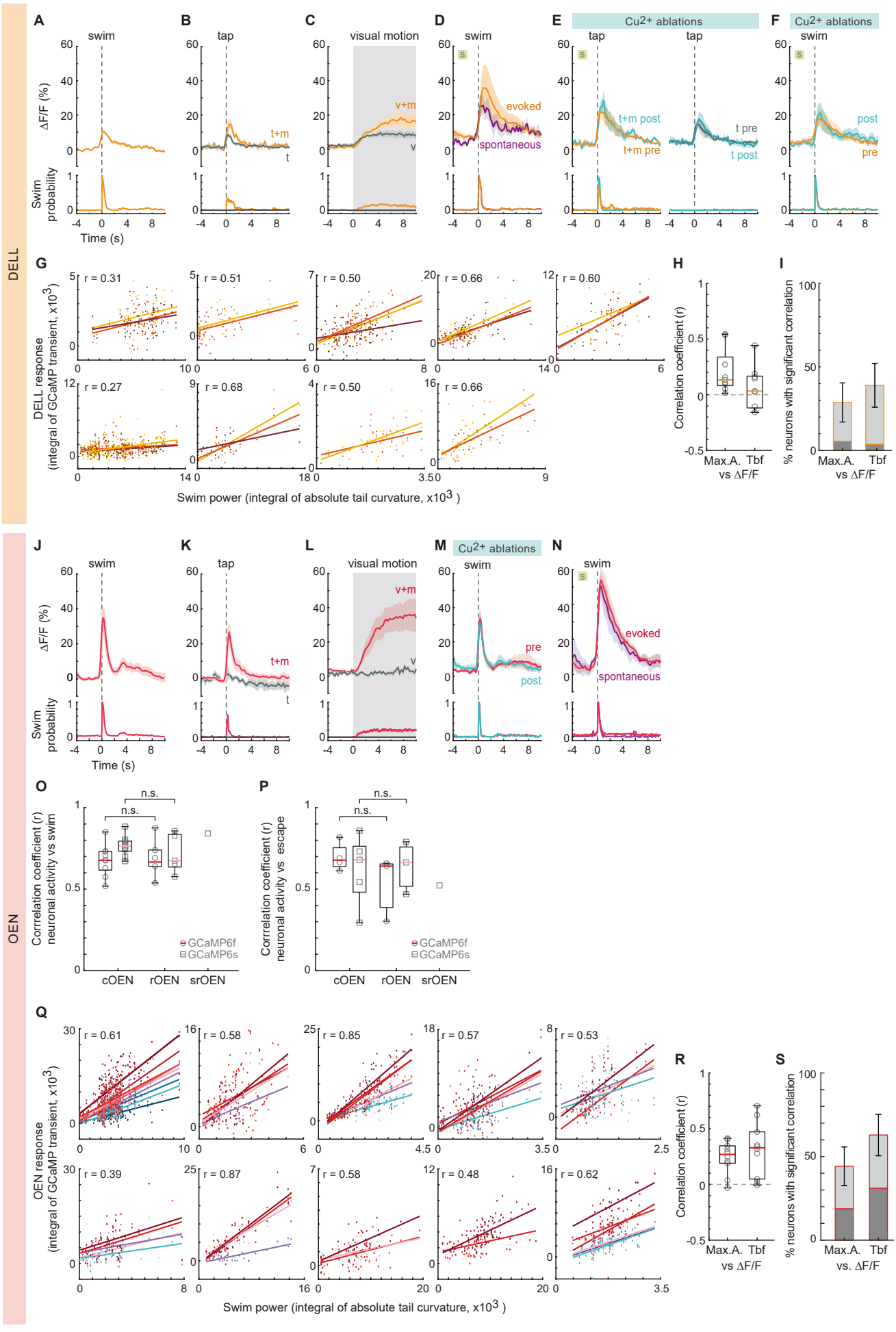
DELL
OEN
A
B
C
D
E
F
G
H
I
J
K
L
M
N
O
P
Q
R
S
swim
tap
visual motion
Cu2+ ablations
ΔF/F (%)
Swim probability
Time (s)
t+m
t
v+m
v
evoked
spontaneous
t+m post
t+m pre
t pre
t post
post
pre
DELL response (integral of GCaMP transient, x10^3)
OEN response (integral of GCaMP transient, x10^3)
Swim power (integral of absolute tail curvature, x10^3)
Correlation coefficient (r)
% neurons with significant correlation
Max.A. vs ΔF/F
Tbf vs ΔF/F
Corrrelation coefficient (r) neuronal activity vs swim
Corrrelation coefficient (r) neuronal activity vs escape
GCaMP6f
GCaMP6s
cOEN
rOEN
srOEN
n.s.

Figure S3. Activity of efferent nuclei during locomotion and in response to diverse sensory stimuli. Related to Figure 3.

Most experiments were performed on fish expressing GCaMP6f. Instances using GCaMP6s animals are signaled by an 'S' on a green square. **(A-F)** Top: Population averages of DELL neuronal activity (mean ΔF/F ± s.e.m.). Bottom: swim probability. **(A)** Average swim-triggered neuronal responses (n= 6 fish). **(B)** Average stimulus-triggered neuronal responses to taps that elicited motor responses (t+m, orange) and taps that did not (t, gray) (n= 5 fish). **(C)** Average stimulus-triggered responses during periods of moving visual gratings that elicited (v+m, orange) and failed to elicit (v, gray) motor responses (n= 8 fish). **(D)** Average swim-triggered neuronal responses after swim bouts that were spontaneous (purple) or evoked by a moving grating (orange) (n= 5 fish). **(E)** Average stimulus-triggered neuronal responses to taps before and after ablation of the lateral line using copper sulfate. Responses are separated depending on whether the tap elicited (left) or did not elicit (right) motor responses (n= 4 fish). **(F)** Average swim-triggered neuronal responses before and after ablation of the lateral line by copper sulfate (n= 6 fish). **(G)** Scatter plots showing the relationship between the power of each individual swim bout versus the intensity of the concurrent neuronal responses of all labeled DELL neurons in each of the 9 fish analyzed. Correlation coefficients and best-fit lines arising from linear regression were calculated for each neuron (shown in different shades), and used to calculate the mean correlation coefficient (r) per fish. Swim power was defined as the integral of the absolute tail curvature trace for individual bouts: a stationary tail has little curvature and thus power is ~0, whereas an undulating tail has a positive absolute tail curvature, which increases as a function of motor strength. Neuronal activity was defined as the integral of the calcium transient during each corresponding bout. **(H)** Box plots showing the mean Pearson's coefficients correlating maximum tail amplitude (Max. A.) or tail beat frequency (Tbf) of single bouts with the concurrent neuronal activity of DELL neurons in individual fish (gray circles, n= 9 fish). Median shown in color. **(I)** Mean percentage of DELL cells per fish whose activity was significantly correlated with maximum tail amplitude or tail beat frequency (n= 9 fish, dark gray $p < 0.001$, light gray < 0.05, error bars: s.e.m). **(J-N)** Top: Population averages of OEN neuronal activity (mean ΔF/F ± s.e.m.). Bottom: swim probability. **(J)** Average swim-triggered neuronal responses (n= 9 fish). **(K)** Average stimulus-triggered neuronal responses to taps that elicited motor responses (t+m, red) and taps that did not (t, gray) (n= 5 fish). **(L)** Average stimulus-triggered responses during periods of moving visual gratings that elicited (v+m, red) and failed to elicit (v, gray) motor responses (n= 10 fish). **(M)** Average swim-triggered neuronal responses before and after ablation of the lateral line by copper sulfate (n= 6 fish). **(N)** Average swim-triggered neuronal responses after swim bouts that were spontaneous (purple) or evoked by a moving grating (red) (n= 7 fish). **(O)** Boxplots of mean Pearson's coefficients relating swimming behavior and neuronal activity (ΔF/F) in different OEN subnuclei of fish expressing GCaMP6f (circles, c=9, r=6) or 6s (squares, c=8, r=5, sr=1). Medians shown in color. Locomotor behavior was convolved with a calcium kernel to account for calcium dynamics. (Pearson's correlation, $p<0.001$; 2-tailed Wilcoxon rank-sum test, p= 0.86 and 0.52 for GCaMP6f and 6s, respectively.) **(P)** Boxplots of mean population Pearson's coefficients relating short-latency escape behaviors and neuronal activity (ΔF/F) in different OEN subnuclei of fish expressing GCaMP6f (circles, c=5, m=3) or 6s (squares, c=5, r=3, sr=1). Median shown in color. Locomotor behavior was convolved with a calcium kernel to account for calcium dynamics. (Pearson's correlation, $p<0.001$; 2-tailed Wilcoxon rank-sum test, p= 0.23 and 0.99 for GCaMP6f and 6s, respectively.) **(Q)** Scatter plots showing the relationship between the power of all individual swim bouts versus the neuronal responses of all labeled OEN neurons in each of the 10 fish analyzed. Correlation coefficients and best-fit lines arising from linear regression were calculated for each neuron (shown in different shades), and used to calculate the mean correlation coefficient (r) per fish. **(R)** Box plots of mean Pearson's coefficients correlating maximum tail amplitude (Max.A.) or tail beat frequency (Tbf) of single bouts with the concurrent neuronal activity of OEN neurons of individual fish (gray squares, n= 10 fish). Median shown in color. **(S)** Mean percentage of OEN cells per fish whose activity was significantly correlated with maximum tail amplitude or tail beat frequency (n= 10 fish, dark gray $p < 0.001$, light gray < 0.05, error bars: s.e.m).

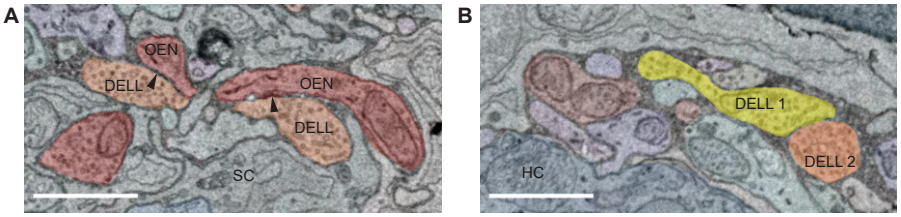

Figure S4. ssEM images of efferent to efferent connections in a posterior lateral line neuromast. Related to Figure 4.
(A) DELL vesicle-filled profiles in close apposition to an OEN axon (arrowheads), surrounded by a support cell (SC).
(B) Vesicle-filled profiles from two separate DELL neurons contact each other. A hair cell (HC) is also labeled for reference. Scale bars: 1 μm.

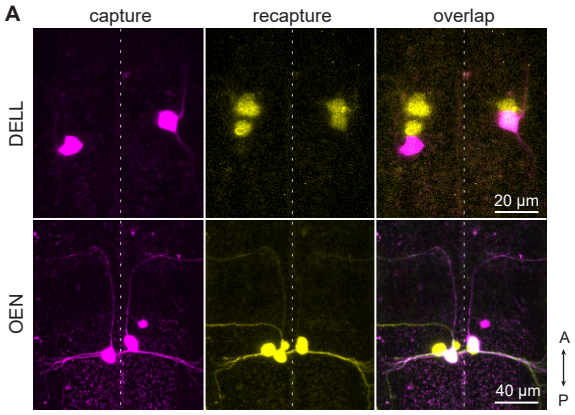

B

Efferent nucleus	Population estimate (unilateral)	Maximum labeled	n
DELL	3.02 ± 1.13	5	48
srOEN	1.00 ± 0.00	1	2
rOEN	1.86 ± 0.84	3	25
cOEN	2.66 ± 1.25	5	43

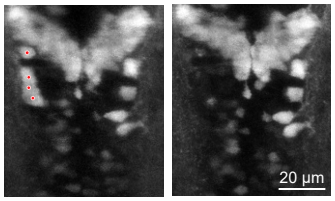

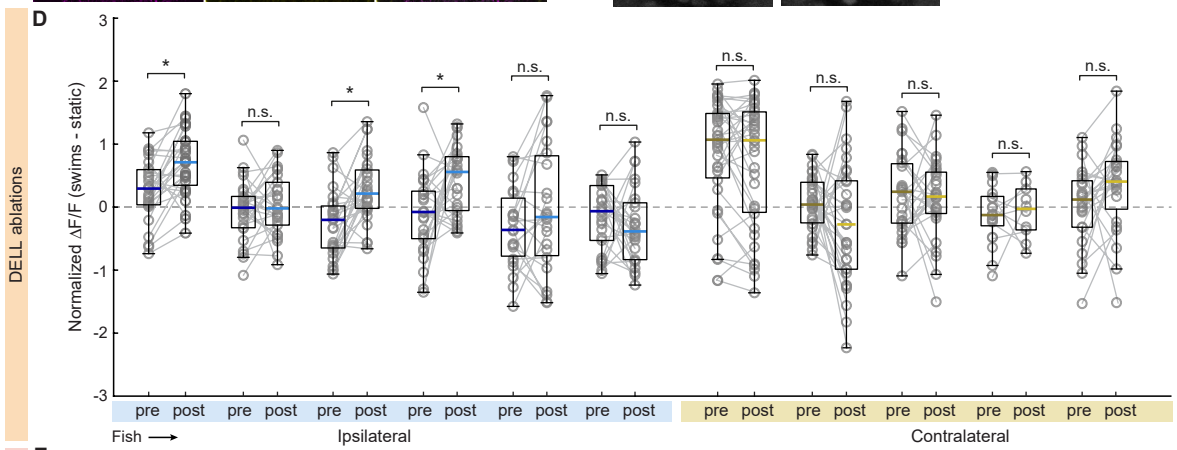

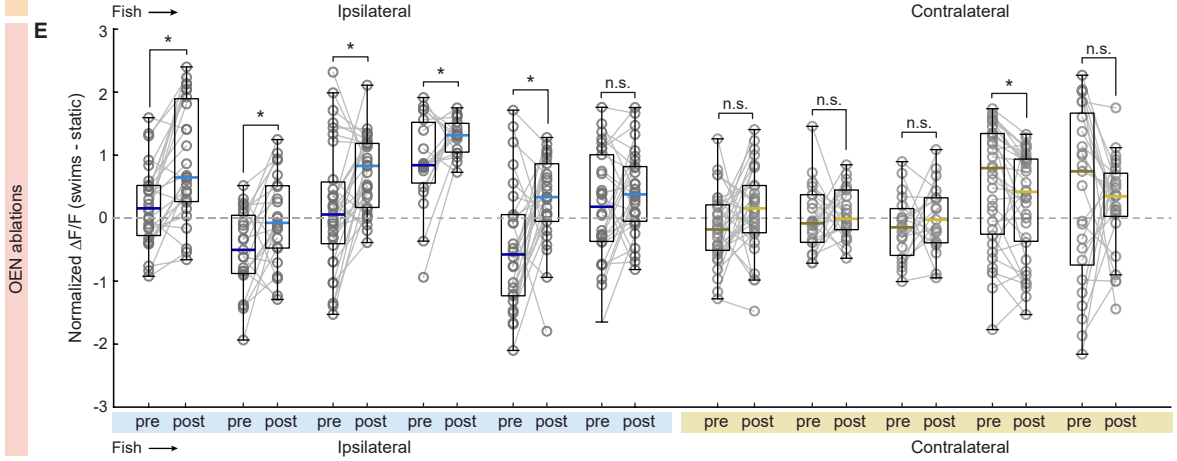

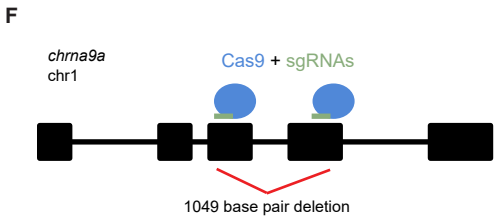

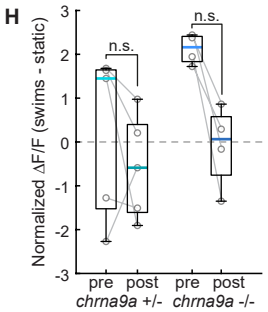

G

```
chrna9a       MEGYSNALRPVEDTDKALNVTLQITLSQIKDMDERNQVLTTYLWVRQIWHDAYLSWDKEEYDGLEVIRIPSNLVWRPDIVLYNNADEEDSSGPPDTNVVLRYNGEITWDSPAITKSSCKV
chrna9Δ1049   MEGYSNALRPVEDTDKALNVTLQITLSQIKDMDERNQVLTTYLWVRQIWHDAYLSWDKEEYDGLEVIRIPSNLVWRPDIVLYNNADEEDSSGPPDTGYGPAGSDCISADGS--------

chrna9a       DVSYFPFDSQECNLTFGSWTYNGNQVDIAMGMESGDLSDFVDNVEWECHGMPAVKNVIMYGCCSDPYPDITYTVLLKRRSSFYIFNLLLPCFLISFLAPLGFYLPADSGEKVSLGVTVLL
chrna9aΔ1049  ----------------------------------------------------------------------------------------------------------------------------

chrna9a       ALTVFQLMVAESMPPSESVPLIGKYYIATMTMITASTSLTIFIMNIHFCGAEAKPVPHWAKVLIIDYMSKIFFVYEVGENCTTPESDRGPFFSEDPLASLERDGYFDKGFYEDCHLDERI
chrna9aΔ1049  ----------------------------------------------------------------------------------------------------------------------------

chrna9a       RSQFNGYSHRDHRHGNGYHHKNSSYRQHRNEQQRRTRSSSNSPVRQSSHHPKYTHFIGRDGSEKLPLTSQEKLKDSEISIPEKINGYTYDQGNGYLNGVGYLHDNGYSKTFGADSYNKTT
chrna9aΔ1049  ----------------------------------------------------------------------------------------------------------------------------

chrna9a       TGTGCVCGKHQKLVRNIEYIANCFREQRGHQAKGAEWKKVAKVMDRFFMWVFFIMVFLMSILVLAKAT
chrna9aΔ1049  ------------------------------------------------------------------
```

Figure S5. Efferent nuclei size estimation, effects of efferent nuclei laser ablation on PLLg activity and generation of mutants lacking α9-nAChRs. Related to Figure 5.

(A) Dorsal projections of confocal images of fish that underwent consecutive dye injections of the lateral line nerve to estimate efferent population size. Top: DELL neurons, bottom: OEN neurons. **(B)** Estimated number of neurons comprising each efferent nucleus innervating the PLL. **(C)** Dorsal projections of confocal images of DELL neurons before and after laser ablations. Red dots indicate targeted neurons. **(D-E)** Boxplots of z-scored ΔF/F showing the difference in activity during swimming and quiescent periods of single neurons in PLL ganglia located ipsilaterally (blue) or contralaterally (yellow) to the ablation site. Medians shown in color. **(D)** Differences were computed for each neuron before and after DELL ablations. Paired 2-tailed Wilcoxon signed-rank test: $p_{ipsilateral}$= 0.3257,0.0714, 0.8854, 0.9219, 0.0814, $p_{contralateral}$= 0.0014, 0.3673, 0.0014, 0.0107, 0.2238, 0.3158. **(E)** Differences were computed for each neuron before and after OEN ablations. Paired 2-tailed Wilcoxon signed-rank test: $p_{ipsilateral}$= $9.994x10^{-4}$, 0.0089, 0.0057, 0.0269, 0.0107, 0.1714, $p_{contralateral}$= 0.0524, 0.6378, 0.3547, 0.0032, 0.5449. **(F)** Diagram of the *chrna9a* gene highlighting the CRISPR-Cas9 target sites in exons 3 and 4 and the 1049 base pair region deleted in the mutant. Introns are depicted as thin lines. **(G)** Predicted amino acid sequence of the wild-type Chrna9a and mutant Chrna9aΔ1049 proteins. Shared sequences are highlighted in gray and amino acids changed due to frameshift in red. **(H)** Boxplots of z-scored population ΔF/F per fish showing the difference in neuronal activity during swimming and quiescent periods in mutant animals before and after lateral line ablation with copper sulfate. Medians shown in color. Paired 2-tailed Wilcoxon signed-rank test: $p_{+/-}$= 0.4375, $p_{-/-}$= 0.1250.